September 7, 2017

# Implementing the CFG Model in CCQE Neutrino-Nucleus Scattering

Joseph Wieske
Wayne State University

Advisor
Gil Paz
Wayne State University

## I Abstract

In the past, charged current quasielastic (CCQE) neutrino-nucleus scattering data from the MiniBooNE experiment was analyzed assuming the Relativistic Fermi Gas (RFG) nuclear model [1]. Experiments suggest that nucleons in CCQE scattering can have high-momentum tails in their distribution. This effect is not accounted for in the RFG model, but *is* accounted for in the Correlated Fermi Gas (CFG) model [4]. This paper will detail the process of implementing the CFG model to CCQE neutrino-nucleus scattering data. Before the CFG model may be applied, a current Mathematica code must be modified to account for extra regions in the nucleon momentum distribution that result from the inclusion of the high-momentum tail. The dozen or so different possible kinematic cases for neutrino-nucleus scattering are addressed, compared to the single case of the RFG model.

## II Introduction

MiniBoone is a particle detector at Fermilab which was constructed for the objective of observing a phenomenon known as neutrino oscillations, wherein neutrinos of one lepton flavor "oscillate" to another lepton flavor while in flight. The signal interaction used to detect these oscillations is CCQE neutrino-nucleus scattering,

$$\nu_\mu + n \to \mu^- + p \tag{1}$$
$$\overline{\nu}_\mu + p \to \mu^+ + n \tag{2}$$

where a neutrino (anti-neutrino) collides with a nucleon to produce another nucleon and that neutrino's characteristic charged lepton (anti-lepton). The evidence for neutrino oscillations is that muon neutrinos are sent to a detector and electrons appear, suggesting that the muon neutrinos change flavor to electron neutrinos and produce electrons when they scatter.

When studying neutrino oscillations an understanding of CCQE neutrino-nucleus scattering is imperative. Multiple levels of interactions are present within CCQE scattering. At the deepest level, neutrinos and quarks have interactions described by the standard model. Going up a level, individual nucleons require form factors. Another level up, a nuclear model is needed to describe the behavior of nucleons in the nucleus. Because of this, the cross section is determined by the combination of form factors and a nuclear model, as described below.

The form factors describe the behavior of individual nucleons, with the axial form factor having the largest contribution to the cross section. The MiniBooNE Collaboration used an axial dipole form factor to analyze CCQE data in [2]. Future analysis plans to use the "$z$-expansion" technique for this axial form factor employed in [3]:

$$F_A(q^2) = \sum_{k=0}^{\infty} a_k z(q^2)^k, \tag{3}$$

where $q^2$ is the transfer of four-momentum during scattering.

The nuclear model describes how nucleons interact within the nucleus. Current theory uses the RFG nuclear model, where we will instead use the CFG nuclear model. Motivation for the change in nuclear models is that experiments show that tensor force induced short-range correlations between proton-neutron pairs shift nucleons to high-momentum in symmetric nuclear matter (Ref. [4]). The RFG nuclear model treats nucleon momentum distribution as a step function that drops to zero at the fermi momentum boundary, and *does not* take these shifts into account, see Figure 1.

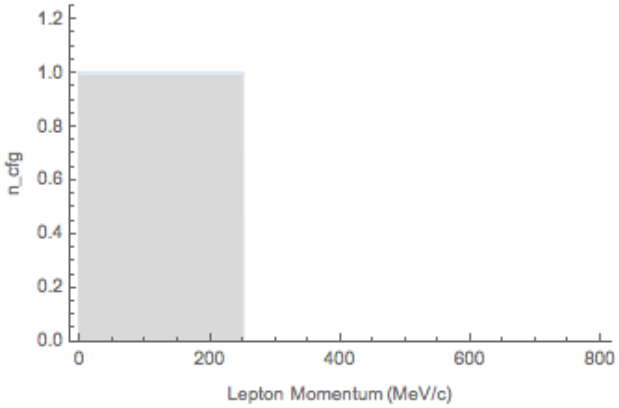


Figure 1: A plot of the RFG nuclear model momentum distribution; the drop takes place at the fermi momentum boundary.

The CFG nuclear model, however, *does* account for these shifts. Instead of dropping to zero at the fermi momentum like the RFG model's distribution does, the CFG model's distribution has a "high-momentum tail" beyond the fermi momentum boundary which falls off as $\frac{1}{|\mathbf{p}|^4}$, where $\mathbf{p}$ is momentum, see Figure 2.

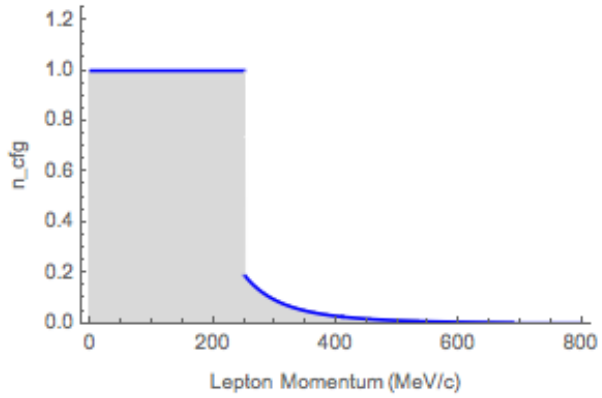


Figure 2: A plot of the CFG nuclear model momentum distribution; note the high-momentum tail beyond the fermi momentum boundary of the RFG.

A current Mathematica code is formatted to utilize the $z$-expansion from [3] and assumes the RFG nuclear model to analyze CCQE scattering data from MiniBoone. In order to analyze data assuming the CFG nuclear model, analytic expressions related to the CFG model's momentum distribution calculated in [7] must be implemented into the code.

# III The Correlated Fermi Gas Model

As seen in Figure 3 below, the CFG momentum distribution contains 4 regions. The case where $\lambda = 1$ would eliminate regions II and III, thus simplifying to the RFG model. In this sense, calculations involving the RFG model need only incorporate the regional transition I→IV. Calculations involving the CFG model must incorporate four regional transitions: I→III, II→III, I→IV, and II→IV.

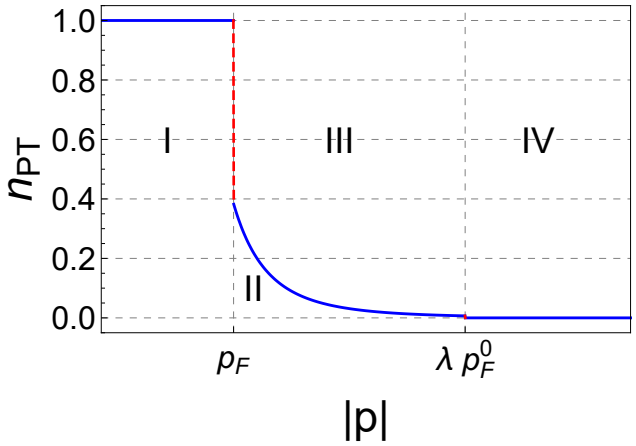


Figure 3: The CFG momentum distribution with respect to the fermi momentum, $p_F$, and the cutoff for the high-momentum tail, $\lambda p_F^0$, where $\lambda > 1$.

The nuclear model's contribution to the CCQE scattering cross section is determined by a set of equations ($a_i$) which are integrated over nucleon energy ($E_P$). Each region has seven of these corresponding $a_i's$ that may be defined in terms of a general-form integral. Because the RFG model only encompasses the I→IV transition, there are just seven $a_i's$ associated with it. The CFG however encompasses four transitions, and therefore has 28 $a_i's$ associated with it. The general-form integral for these equations, derived in [7], is as follows:

$$\begin{aligned}
\tilde{b}(j,k) &= \frac{m_T V}{2\pi|\mathbf{q}|}\left(\frac{c_0 p_F}{A_0}\right)^k \int \frac{E_{\mathbf{p}} dE_{\mathbf{p}}}{(E_{\mathbf{p}}-\epsilon_b)(E_{\mathbf{p}}^2-m_N^2)^{2k}}\left(\frac{E_{\mathbf{p}}}{m_N}\right)^j , && (4)\\
&= \frac{m_T V}{2\pi|\mathbf{q}|m_N^j}\left(\frac{c_0 p_F}{A_0}\right)^k \int \frac{E_{\mathbf{p}}^{1+j} dE_{\mathbf{p}}}{(E_{\mathbf{p}}-\epsilon_b)(E_{\mathbf{p}}^2-m_N^2)^{2k}} , && (5)
\end{aligned}$$

where $m_T$ is the mass of the target nucleon, $m_N$ is the average mass of the proton and neutron, $V$ and $A_0$ are normalization constants, $c_0$ is a constant related to the phenomenological height factor, $\epsilon_b$ is the nucleon binding energy, $|\mathbf{q}|$ is the three-momentum transfer, and $(j,k) = 0,1,2$. The $a_i's$ for the I→IV transition defined in terms of $\tilde{b}(j,k)$ are as follows:

$$\begin{aligned}
a_1(\mathrm{I}\to\mathrm{IV}) &= \tilde{b}(0,0) , && (6)\\
a_2(\mathrm{I}\to\mathrm{IV}) &= \tilde{b}(2,0) - \tilde{b}(0,0) , && (7)\\
a_3(\mathrm{I}\to\mathrm{IV}) &= c^2\tilde{b}(2,0) + 2cd\tilde{b}(1,0) + d^2\tilde{b}(0,0) , && (8)\\
a_4(\mathrm{I}\to\mathrm{IV}) &= \tilde{b}(2,0) - 2\frac{\epsilon_b}{m_N}\tilde{b}(1,0) + \frac{\epsilon_b^2}{m_N^2}\tilde{b}(0,0) , && (9)\\
a_5(\mathrm{I}\to\mathrm{IV}) &= -c\tilde{b}(2,0) + \left(\frac{\epsilon_b}{m_N}c - d\right)\tilde{b}(1,0) + \frac{\epsilon_b}{m_N}d\tilde{b}(0,0) , && (10)\\
a_6(\mathrm{I}\to\mathrm{IV}) &= -c\tilde{b}(1,0) - d\tilde{b}(0,0) , && (11)\\
a_7(\mathrm{I}\to\mathrm{IV}) &= \tilde{b}(1,0) - \frac{\epsilon_b}{m_N}\tilde{b}(0,0) , && (12)
\end{aligned}$$

where $\omega_{\mathrm{eff}}$ is the difference between the energy of the incident neutrino, the resulting lepton, and $\epsilon_b$, and $c = -\omega_{\mathrm{eff}}/|\mathbf{q}|$ and $d = -(\omega_{\mathrm{eff}}^2 - |\mathbf{q}|^2)/(2|\mathbf{q}|m_N)$ have been used to simplify the expressions. If we denote the linear combination of $\tilde{b}'s$ as $f_i(\tilde{b}(j,k))$ such that $a_i(\mathrm{I}\to\mathrm{IV}) = f_i(\tilde{b}(j,k=0))$, then the form of the $a_i's$ for all transitions may be written as

$$\begin{aligned}
a_i(\mathrm{I}\to\mathrm{IV}) &= f_i(\tilde{b}(j,k=0)) , && (13)\\
a_i(\mathrm{II}\to\mathrm{IV}) &= f_i(\tilde{b}(j,k=1)) , && (14)\\
a_i(\mathrm{I}\to\mathrm{III}) &= a_i(\mathrm{I}\to\mathrm{IV}) - a_i(\mathrm{II}\to\mathrm{IV}) ,\\
&= f_i(\tilde{b}(j,k=0)) - f_i(\tilde{b}(j,k=1)) , && (15)\\
a_i(\mathrm{II}\to\mathrm{III}) &= a_i(\mathrm{II}\to\mathrm{IV}) - f_i(\tilde{b}(j,k=2)) ,\\
&= f_i(\tilde{b}(j,k=1)) - f_i(\tilde{b}(j,k=2)) . && (16)
\end{aligned}$$

# IV Limits of Integration

Kinematics from a CCQE scattering event, such as the scattering angle and energy of the resulting characteristic lepton, may be used to determine the range of integration for these equations. Physical restraints on the kinematic variables and the boundary conditions for each of the four regions (see Figure 3) are used to determine the upper ($E_{\rm hi}$) and lower limits ($E_{\rm lo}$) of integration for each transition (derived in [7]). From Eq.'s (17) - (23), we see that the limits of integration for all four transitions depend on the numerical relations between 5 parameters: $E_F$, $E_F - \omega_{\rm eff}$, $E_F^\lambda$, $E_F^\lambda - \omega_{\rm eff}$, and $\Delta \equiv m_N \frac{cd + \sqrt{1 - c^2 + d^2}}{1 - c^2}$. $E_F$ is the fermi energy associated with the fermi momentum, $E_F = \sqrt{m_N^2 + p_F^2}$. $E_F^\lambda$ is the cutoff energy associated with the high-momentum tail cutoff in the CFG nuclear model's momentum distribution, $E_F^\lambda = \sqrt{(\lambda p_F)^2 + m_N^2}$. The $\Delta$ term is derived in the appendix of Ref. [1] as a result of the delta function and the condition that $-1 \leq \cos\theta \leq 1$ for a physical scattering angle $\theta$. Note that if the kinematics for a specific instance of CCQE scattering yield values for the 5 parameters such that $E_{\rm hi} \leq E_{\rm lo}$ for one of the regional transitions, then that transition will not contribute to the cross section. The limits are determined as follows:

**I $\rightarrow$ IV:** For the I $\rightarrow$ IV transition the initial energy of the nucleon must be less than or equal to the Fermi energy, otherwise it wouldn't be within region I. The Fermi energy must be less than $E_F^\lambda$ which must be less than or equal to the final energy of the nucleon ($E_{\mathbf{p+q}}$).

$$\begin{aligned} \text{I} \rightarrow \text{IV}: \; E_{\mathbf{p}} \;\leq\; E_F \;<\; E_F^\lambda \;\leq\; E_{\mathbf{p+q}} \;=\; E_{\mathbf{p}} + \omega_{\rm eff} \;, \\ \Rightarrow \; \min(E_F, E_F^\lambda - \omega_{\rm eff}) \;\leq\; E_{\mathbf{p}} \;, \\ E_{\rm lo} = max(E_F^\lambda - \omega_{\rm eff}, \Delta) \;, \\ E_{\rm hi} = E_F \;. \end{aligned} \tag{17}$$

(18)

**II $\rightarrow$ IV:** For the II $\rightarrow$ IV transition the initial energy of the nucleon must be greater than the Fermi energy, but still less than $E_F^\lambda$, otherwise it wouldn't be within region 2. The final energy of the nucleon must be greater than $E_F^\lambda$ to ensure that the nucleon gained enough energy to enter region IV.

$$\begin{aligned} \text{II} \rightarrow \text{IV}: \quad E_F \;\leq\; E_{\mathbf{p}} \;\leq\; E_F^\lambda \;\leq\; E_{\mathbf{p+q}} \;=\; E_{\mathbf{p}} + \omega_{\rm eff} \;, \\ \Rightarrow \; \max(E_F, E_F^\lambda - \omega_{\rm eff}) \;\leq\; E_{\mathbf{p}} \;, \\ E_{\rm lo} = max(E_F, E_F^\lambda - \omega_{\rm eff}, \Delta) \;, \\ E_{\rm hi} = E_F^\lambda \;. \end{aligned} \tag{19}$$

(20)

**I → III:** For the I → III transition the initial energy of the nucleon must be less than or equal to the Fermi energy, otherwise it wouldn't be within region I. The final energy of the nucleon must then be greater than the Fermi energy, but less than $E_F^\lambda$. These boundary conditions establish that the nucleon ends up in region III.

$$\begin{aligned} \text{I} \rightarrow \text{III}: \quad & E_{\mathbf{p}} \;\leq\; E_F \;\leq\; E_{\mathbf{p}+\mathbf{q}} \;=\; E_{\mathbf{p}} + \omega_{\text{eff}} \;\leq\; E_F^\lambda \;, \qquad (21) \\ & \Rightarrow\; E_F - \omega_{\text{eff}} \leq E_{\mathbf{p}} \;\leq\; E_F^\lambda - \omega_{\text{eff}} \;, \\ & E_{\text{lo}} = max(E_F - \omega_{\text{eff}}, \Delta) \;, \\ & E_{\text{hi}} = min(E_F^\lambda - \omega_{\text{eff}}, E_F) \;. \end{aligned}$$

(22)

**II → III:** For the II → III transition the initial energy of the nucleon must be greater than the Fermi energy, but still less than the final energy of the nucleon, which is less than $E_F^\lambda$. This keeps the nucleon within the bounds of regions II and III, but limits the initial energy to be less than the final energy. Note that when $\omega_{\text{eff}}$ is negative, contributions will result only from the II → III transition, if at all. Looking at Figure 3, this transition can be visualized as an arrow that begins in the tail end of region II and points backwards and up into region III.

$$\begin{aligned} \text{II} \rightarrow \text{III}: \quad & E_F \;\leq\; E_{\mathbf{p}} \;<\; E_{\mathbf{p}+\mathbf{q}} \;=\; E_{\mathbf{p}} + \omega_{\text{eff}} \;\leq\; E_F^\lambda \;, \qquad (23) \\ & \Rightarrow\; E_F \;\leq\; E_{\mathbf{p}} \;\leq\; E_F^\lambda - \omega_{\text{eff}} \;, \\ & E_{\text{lo}} = max(E_F, \Delta) \;, \\ & E_{\text{hi}} = min(E_F^\lambda - \omega_{\text{eff}}, E_F^\lambda) \;. \end{aligned}$$

# V Ordering of Parameters

Because the numerical relations above depend on 5 parameters, there are $5! = 120$ permutations possible. However, these parameters are subject to physical and logical constraints which greatly reduce the number of permutations that may actually be obtained. Because $E_F$ and $E_F^\lambda$ are functions of constants ($p_F$ and $m_N$), $\lambda > 1$ implies that $E_F < E_F^\lambda$ must always hold. Similarly, it must always hold that $E_F - \omega_{\text{eff}} < E_F^\lambda - \omega_{\text{eff}}$. These two requirements alone reduce the number of valid permutations to 30. For consistency, it must simultaneously hold that $E_F < E_F - \omega_{\text{eff}}$ and $E_F^\lambda < E_F^\lambda - \omega_{\text{eff}}$ in the case that $\omega_{\text{eff}}$ is negative, and that $E_F > E_F - \omega_{\text{eff}}$ and $E_F^\lambda > E_F^\lambda - \omega_{\text{eff}}$ in the case of a positive $\omega_{\text{eff}}$. This requirement further reduces the number of valid transitions to 20.

Noting also from Eq.'s (17) - (23), $\Delta$ is present in the expression for the lower limit of integration in each of the four transitions. Since the expressions for $E_{\text{lo}}$ take the maximum of an argument, any instance where $\Delta$ is greater than the other four parameters will yield $E_{\text{hi}} \leq E_{\text{lo}}$ for all transitions. As mentioned in the previous section, any transition for which $E_{\text{hi}} \leq E_{\text{lo}}$ will have no contribution; therefore we also apply the constraint that the maximum of the five parameters may not be $\Delta$. In a similar fashion, the expressions for the limits of

integration are such that any case in which $E_F < E_F^\lambda < \Delta$ will have no contribution from any transition. These two requirements remove 7 more permutations, bringing the total number of valid permutations to 13.

Table 1: Constants used in calculations for limits of integration. See [4] for $p_F$ and $\lambda$, see [5] for $\epsilon_b$, and see [6] for $m_\mu$ and $m_n$.

| $p_F$(GeV) | $\lambda$ | $\epsilon_b$(GeV) | $m_\mu$(GeV/$c^2$) | $m_N$(GeV/$c^2$) | $E_F$(GeV) | $E_F^\lambda$(GeV) |
|---|---|---|---|---|---|---|
| 0.250 | $2.75 \pm 0.25$ | 0.025 | 0.1057 | 0.9389 | 0.972 | 1.164 |

The data gathered from MiniBooNe dealt with incident neutrino energies ranging from 50 MeV to 3 GeV and resulting lepton energies ranging from 0.2 GeV to 2 GeV (Ref [2]). When dealing with these ranges, the $\Delta$ term appears to have an absolute minimum value of approximately 0.94 GeV. The case $\Delta < E_F - \omega_{\text{eff}} < E_F^\lambda - \omega_{\text{eff}} < E_F < E_F^\lambda$ is prevented from ever occurring due to this minimum, because the fixed values of $E_F$ and $E_F^\lambda$ along with the overall ordering of the parameters would require $\Delta$ to take values significantly less than 0.94 GeV (see Table 1 above). The case $\Delta < E_F < E_F^\lambda < E_F - \omega_{\text{eff}} < E_F^\lambda - \omega_{\text{eff}}$ is also unobtainable when dealing with MiniBoone kinematics. The linear dependence between the parameters in this permutation places a local minimum value on $\Delta$ of approximately 1.12 GeV; this contradicts $\Delta < E_F$ because $E_F = 0.972$ GeV $< 1.12$ GeV. These two final restrictions leave just 11 valid permutations of the original 120. Listed exhaustively, they are:

$$1 : \quad \Delta < E_F - \omega_{\text{eff}} < E_F < E_F^\lambda - \omega_{\text{eff}} < E_F^\lambda \ , \tag{24}$$
$$2 : \quad E_F - \omega_{\text{eff}} < \Delta < E_F < E_F^\lambda - \omega_{\text{eff}} < E_F^\lambda \ , \tag{25}$$
$$3 : \quad E_F - \omega_{\text{eff}} < E_F < \Delta < E_F^\lambda - \omega_{\text{eff}} < E_F^\lambda \ , \tag{26}$$
$$4 : \quad E_F - \omega_{\text{eff}} < E_F < E_F^\lambda - \omega_{\text{eff}} < \Delta < E_F^\lambda \ , \tag{27}$$
$$5 : \quad E_F - \omega_{\text{eff}} < \Delta < E_F^\lambda - \omega_{\text{eff}} < E_F < E_F^\lambda \ , \tag{28}$$
$$6 : \quad E_F - \omega_{\text{eff}} < E_F^\lambda - \omega_{\text{eff}} < \Delta < E_F < E_F^\lambda \ , \tag{29}$$
$$7 : \quad E_F - \omega_{\text{eff}} < E_F^\lambda - \omega_{\text{eff}} < E_F < \Delta < E_F^\lambda \ , \tag{30}$$
$$8 : \quad \Delta < E_F < E_F - \omega_{\text{eff}} < E_F^\lambda < E_F^\lambda - \omega_{\text{eff}} \ , \tag{31}$$
$$9 : \quad E_F < \Delta < E_F - \omega_{\text{eff}} < E_F^\lambda < E_F^\lambda - \omega_{\text{eff}} \ , \tag{32}$$
$$10 : \quad E_F < E_F - \omega_{\text{eff}} < \Delta < E_F^\lambda < E_F^\lambda - \omega_{\text{eff}} \ , \tag{33}$$
$$11 : \quad E_F < \Delta < E_F^\lambda < E_F - \omega_{\text{eff}} < E_F^\lambda - \omega_{\text{eff}} \ . \tag{34}$$

# VI Implementation to Code

In order to analyze scattering data using the CFG nuclear model, code must be written that determines which of the four regional transitions yield valid contributions, calculates the corresponding upper and lower limits of integration, and evaluates the $a_i's$. This task is simplified when using the RFG nuclear model, which effectively only takes the I→IV

transition into consideration. The upper limit of integration is fixed for this transition, and the lower limit is the maximum of two parameters; either the contribution will come entirely from this transition, or there will be no contribution at all. When using the CFG, contributions may come from any combination of the four transitions, each with different limits of integration and integrals to determine and calculate, where each limit has its own expression.

To illustrate how the four transitions may (or may not) contribute, consider case 1 : $\Delta < E_F - \omega_{\text{eff}} < E_F < E_F^\lambda - \omega_{\text{eff}} < E_F^\lambda$; if we "plug in" this ordering of the parameters to the expressions for the limits of integration (Eq.'s (17) - (23)), we obtain the results in Table 2.

Table 2: Values for the limits of integration for the ordering of the 5 parameters in case 1.

| Transition | I→IV | II→IV | I→III | II→III |
|---|---|---|---|---|
| $E_{\text{lo}}$ | $E_F^\lambda - \omega_{\text{eff}}$ | $E_F^\lambda - \omega_{\text{eff}}$ | $E_F - \omega_{\text{eff}}$ | $E_F$ |
| $E_{\text{hi}}$ | $E_F$ | $E_F^\lambda$ | $E_F$ | $E_F^\lambda - \omega_{\text{eff}}$ |

From Table 1, the difference between $E_F$ and $E_F^\lambda$ is approximately 0.19 GeV. For $E_F < E_F^\lambda - \omega_{\text{eff}} < E_F^\lambda$ to hold, it must be that $-0.19$ GeV $< \omega_{\text{eff}} < 0$. Thus for case 1 we see that there are valid contributions from all transitions except I→IV, where $E_{\text{lo}} > E_{\text{hi}}$. Therefore, if data for a specific scattering event is used to calculate the 5 parameters and they are in the configuration of case 1, then we know exactly which transitions will yield contributions and exactly what the limits of integration for those transitions will be.

The same process may be repeated for the remaining 10 cases, such that for all 11 cases we will know which transitions matter and what their limits of integration will be. These transitions and limits may be hard-coded for each case, so that the only task required by the code when analyzing data is to evaluate and sort the 5 parameters based on the kinematics of the scattering event being analyzed. The order of the 5 parameters will determine the case which is present, and then values for the limits of integration may be passed in so that the $a_i's$ may be calculated. In this way, the CFG model may be integrated into the Mathematica code and assumed when analyzing CCQE data.

Currently, no analysis has been performed yet assuming the CFG model. In the future, code implementing the CFG model will be finalized and optimized to execute in an efficient manner, and then used to analyze the MiniBoone CCQE scattering data. The contents of this paper as well as possible findings from future analysis will be presented at the Conference Experience for Undergraduates at the October 2017 meeting of the APS Division of Nuclear Physics. Future work may also include generalizing the implementation of the CFG model so that it may be applied to other scattering experiments beyond MiniBoone.

# VII Acknowledgments

I would like to thank Jameson Tockstein, Dr. Bhattacharya, and Dr. Paz for their help during this research. I would like to specifically thank Dr. Paz for all of his advice and guidance as my advisor, and for allowing me the opportunity to continue research on this project and attend the October 2017 APS DNP meeting. I would also like to acknowledge the rest of the staff and faculty involved in Wayne State University's 2017 Research Experience for Undergraduates program funded by the National Science Foundation via grant PHY-1460853. This REU has provided me with essential experience in research that I will carry with me through my career in physics, and I am honored to have been a participant.

# References

[1] R. A. Smith and E. J. Moniz, "Neutrino Reactions On Nuclear Targets," Nucl. Phys. B **43**, 605 (1972) Erratum: [Nucl. Phys. B **101**, 547 (1975)] doi:10.1016/0550-3213(75)90612-4, 10.1016/0550-3213(72)90040-5.

[2] A. A. Aguilar-Arevalo et al. [MiniBooNE Collaboration], "First Measurement of the Muon Neutrino Charged Current Quasielastic Double Differential Cross Section," Phys. Rev. D **81**, 092005 (2010) doi:10.1103/PhysRevD.81.092005 [arXiv:1002.2680 [hep-ex]].

[3] B. Bhattacharya, R. J. Hill and G. Paz, "Model independent determination of the axial mass parameter in quasielastic neutrino-nucleon scattering," Phys. Rev. D **84**, 073006 (2011) doi:10.1103/PhysRevD.84.073006 [arXiv:1108.0423 [hep-ph]].

[4] O. Hen, B. A. Li, W. J. Guo, L. B. Weinstein and E. Piasetzky, "Symmetry Energy of Nucleonic Matter With Tensor Correlations," Phys. Rev. C **91**, 025803 (2015) doi:10.1103/PhysRevC.91.025803 [arXiv:1408.0772 [nucl-ex]].

[5] E. J. Moniz, I. Sick, R. R. Whitney, J. R. Ficenec, R. D. Kephart and W. P. Trower, Phys. Rev. Lett. 26, 445 (1971)

[6] K. Nakamura et al. [Particle Data Group], J. Phys. G 37, 075021 (2010)

[7] B. Bhattacharya, J. Tockstein, and G. Paz, "CFG Notes on Limits of Integration," Unpublished.